Electronic-Band-Structure Mapping of Nanotube Transistors by Scanning Photocurrent Microscopy**

Eduardo J. H. Lee, Kannan Balasubramanian, Jens Dorfmüller, Ralf Vogelgesang, Nan Fu, Alf Mews, Marko Burghard,* and Klaus Kern*

Carbon-nanotube field-effect transistors (CNFETs) have been extensively studied for applications in electronics and optoelectronics.[1,2] Despite significant progress in this research field, a range of important device features remain to be fully explored, such as the nature of the metal–nanotube interface.[3] In this context, scanning probe microscopy can provide relevant local information about various devices.[4,5] A technique well-suited to explore the band-structure profile within carbon-nanotube devices is scanning photocurrent microscopy (SPCM), which has so far revealed dominant photocurrent generation at the nanotube–metal contacts.[6–8] SPCM involves the use of a diffraction-limited laser spot obtained from a confocal microscope to illuminate the sample while it is being scanned. The photocur-

rent is acquired as a function of the position of the laser spot and plotted as an image, which, when combined with a simultaneously taken reflection image gives valuable information about the local origin of the generated photoresponse.[6] Here we report the full characterization of CNFETs by SPCM in different charge-transport regimes and under applied bias. Furthermore, we provide evidence that optical excitation of the nanotubes is indeed the origin of the detected photocurrents. The SPCM data enable convenient access to the height of the Schottky barriers at the contacts. Moreover, the obtained band profiles are in excellent agreement with current models of CNTFET device operation.

Figure 1a shows the transfer characteristic of a typical CNFET displaying slightly asymmetric ambipolar behav-
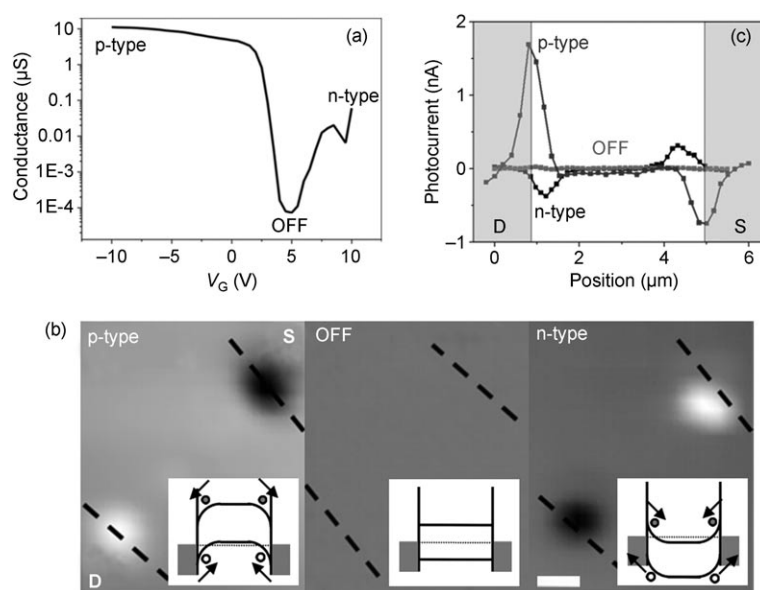

Figure 1. a) Plot of conductance versus gate voltage of a CNFET; b) zero-bias SPCM images (white corresponds to positive current). The dashed lines indicate the edges of the source (S) and drain (D) electrical contacts, and the insets depict the respective band diagrams. c) Photocurrent line profiles taken along the nanotube channel. Scale bar is 1 μm.

[*] E. J. H. Lee, Dr. K. Balasubramanian, J. Dorfmüller,
Dr. R. Vogelgesang, Dr. M. Burghard, Prof. K. Kern
Max-Planck-Institut fuer Festkoerperforschung
Heisenbergstrasse 1, 70569 Stuttgart (Germany)
Fax: (+49) 711-689-1662
E-mail: e.lee@fkf.mpg.de
        m.burghard@fkf.mpg.de
Prof. K. Kern
Institut de Physique des Nanostructures
Ecole Polytechnique Fédérale de Lausanne (EPFL)
1015 Lausanne (Switzerland)
N. Fu, Prof. A. Mews
Physical Chemistry
University of Siegen
Adolf Reichwein Strasse 2, 57068 Siegen (Germany)

Supporting information for this article is available on the WWW under http://www.small-journal.com or from the author.

iour. All samples examined in this study (see Experimental Section) yielded the same qualitative behaviour with and without illumination. The photocurrent images of the device taken at zero source–drain bias in both the p- and n-type regimes, presented in Figure 1b, reveal enhanced photocurrent responses close to the metal contacts. By contrast, no detectable photoresponse is observed along the entire CNFET device in the OFF state. This difference can be explained by Schottky barriers at the contacts prevalent in the ON states, whereas the flat bands in the OFF state do not support acceleration of the photogenerated carriers (see insets of Figure 1b). The gate-induced modulation of the SPCM images solidifies the previous conclusion that built-in electric fields are responsible for the photocurrent generation.[6,7] Further support for such interpretation stems from the sign of the photocurrent lobes in the various regimes, as exemplified by the line profiles in Figure 1c. Based upon the convention that electrons flowing out of the source con-

tact are measured as a positive current, the signs of the photocurrents at the contacts in the ON states of the device are consistent with the direction of the built-in fields there.

Although the photoresponses in the p- and n-type regimes are qualitatively similar, they exhibit subtle differences. While in the p-type regime, the photocurrent peaks appear almost exactly at the tube–contact interface, in the n-type regime they are offset by $\approx 0.25 \, \mu m$ towards the centre of the nanotube channel. Such behaviour was observed in all of the investigated samples. It demonstrates that the band structure of the device in the p-type regime is not just a mirror image of that in the n-type regime. For further elucidation, a series of zero-bias photocurrent images were acquired while sweeping the gate voltage from the n-type regime to the p-type regime, as depicted in Figure 2a. It is apparent that while tuning the device from the n-type regime to the OFF state, the photocurrent lobes shift gradually towards the centre of the channel, become broader, and considerably decrease in intensity. The very low intensity

(few tens of pA) features along the channel in the OFF state, observed for some of the samples, may be ascribed to weak local electric fields similar to those observed in metallic carbon nanotubes.[7] Such fields could arise due to defect sites.[5] When the device is further tuned to the p-type regime, the lobes appear suddenly at the contacts without showing any gradual movements. This observation is independent of the speed and direction of the gate voltage sweep. The trend observed upon switching from the n-type regime to the OFF state is indicative of lowering and widening of the Schottky barriers. These changes are consistent with theoretical simulations, according to which the Schottky-barrier width is closely related to the magnitude of the local electric fields at the contacts.[9] The sudden appearance of the p-type lobes in comparison to the gradual movement and broadening of the n-type lobes evidences that in the former regime the gate voltage has a much weaker effect on the width of the Schottky barriers. The overall behaviour of the CNFET is in close accord with the doped-CNFET

Figure 2. a) Zero-bias photocurrent response upon transition from the n- to p-type regime (scale bar is 1 µm). Color scales were normalized such that white (black) corresponds to the maximum (minimum) detected current; b) band diagrams depicting the intrinsic- and doped-CNFET models; c) gate-voltage dependence of the drain current (dotted curve) and of the intensity of the photocurrent lobes (solid lines). The inset shows the activation barrier energy at zero bias (dots) and the logarithm of the resistance (line) as a function of gate voltage. V_{th} and V_{fb} correspond to the threshold and flat-band voltages, respectively.

model recently proposed by Chen and Fuhrer.[10] It involves chemical p-type doping upon nanotube exposure to ambient conditions, thereby introducing a strong band bending confined to a very small width W_{doped} for p-type operation (Figure 2b).[11] By comparison, in the n-type regime, charge depletion occurs over an effective barrier width W_{eff} of the order of magnitude of the gate oxide thickness t, which can be effectively modulated by the gate voltage. This situation is different from intrinsic CNFETs for which in both regimes the bands are bent over a depletion length $W \approx t$. Within the doping model, the occurrence of the p-type photocurrent lobes at the contacts and the ≈ 0.25-µm shift of the n-type lobes (Figures 1c) and 2a) can be related to the presence of Schottky barriers with respective widths of W_{doped} and W_{eff}. Moreover, the broadening of the lobes upon transition from the n-type regime to the OFF state is attributeable to an increase of W_{eff}, whereas in the p-type regime, the absence of such behaviour indicates that the Schottky barrier width is confined to W_{doped}. It be-
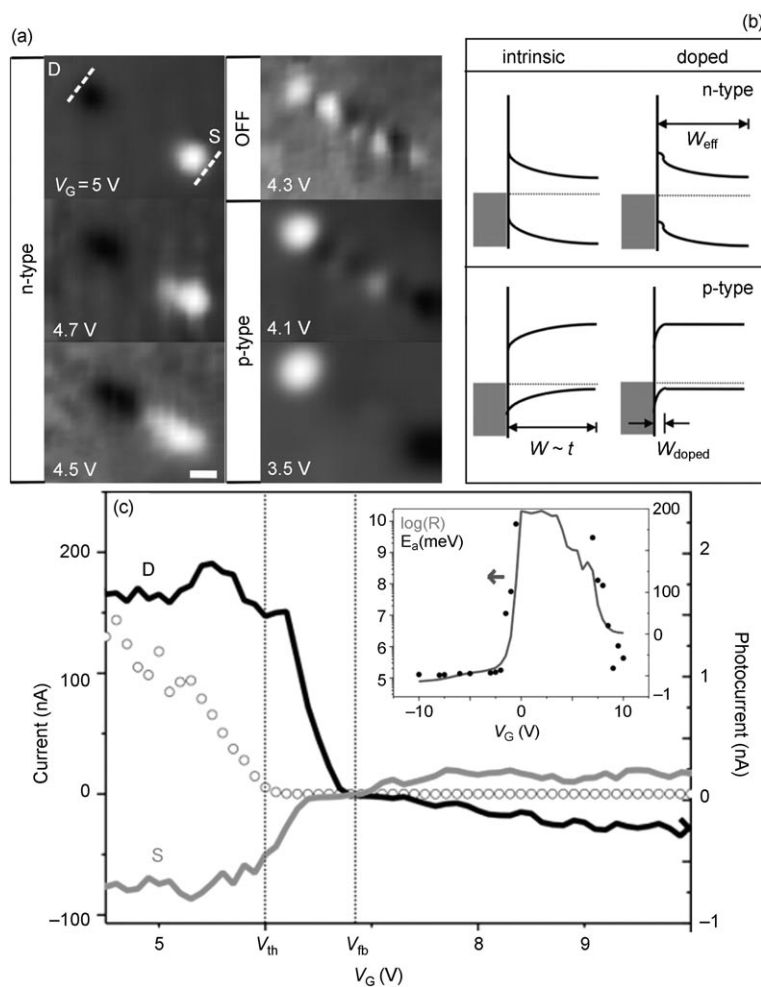
comes thus apparent that the effect of exposure to ambient conditions is not restricted to changes in the metal work function.

Towards the task of determining the band-structure profile of CNFETs with the aid of SPCM it has to be ensured that the observed photocurrent signals originate from photoexcitation of the nanotube. Previous CNFET photoconductivity studies have reported photovoltage generation at the Si–SiO$_2$ interface upon excitation with energies above the Si bandgap.[2,12] To rule out such contributions in the SPCM response, measurements were performed in the p-type regime with laser excitation at $\lambda_{exc} = 1.6\ \mu m$ ($E = 0.78$ eV, 2-μm spot size). The obtained SPCM images displayed the same principal features as in the experiments with $\lambda_{exc} = 633$ nm, proving that the photoresponse predominantly arises from optical excitation of the nanotubes.

In order to determine the Schottky barrier height for holes Φ_{Bp}, the gate dependence of the drain current I_d and the photocurrent at the contacts I_{ph} was evaluated, following a similar procedure as reported for Si nanowires.[13] The two I_{ph} curves in Figure 2c cross each other at $V_G = V_{fb} = 6.9$ V, where I_{ph} is approximately zero. At this gate voltage, the device is in the OFF state with flat bands at the contacts. Moreover, when V_G equals the threshold voltage, the drain current reaches zero, corresponding to the situation where the valence band is approximately aligned at the Fermi level.[14] The Schottky barrier height can be calculated as $\Phi_{Bp} = \alpha \cdot (V_{fb} - V_{th})$, where α is the coupling parameter, which can be estimated from the subthreshold slope obtainable from the drain current curve in the p-type regime.[13,15] For the sample in Figure 2, the subthreshold slope $S = (1/\alpha)(k_B T/e)\ln(10)$ is ≈ 300 mV decade^{-1}, yielding an α value of approximately 0.2, from which Φ_{Bp} is determined to be ≈ 180 meV. Similar values have been obtained for other samples. In order to independently determine Φ_{Bp}, we have performed temperature dependent current–voltage (I–V) measurements and analyzed the data within the framework of thermionic emission theory, as described in previous work.[10,16] The measured activation energy at zero bias is plotted as a function of V_G in the inset of Figure 2c. In the ON states, the activation energy significantly underestimates the barrier height, since charge injection occurs via thermally assisted tunnelling. On the other hand, in the OFF state, thermionic emission is the dominant process, such that the activation energy approaches Φ_{Bp}. Due to sensitivity limitations, a lower limit of ≈ 170 meV is estimated for the barrier height, which is in close agreement to the value obtained by SPCM measurements.

Having characterized the devices at zero bias, we now address the effect of finite drain–source voltage on the band-structure profile of CNFETs. Figure 3a displays a series of SPCM images taken at various bias voltages with the device operated in the n-type regime. Although a somewhat smaller ratio of photocurrent to the dark current is found in the p-type regime, the following discussion applies equally well in this case. The images disclose that an applied voltage leads to the enhancement of one of the photocurrent lobes, depending on the sign of the bias. For sufficiently large bias, a single lobe is observed. To better visualize the
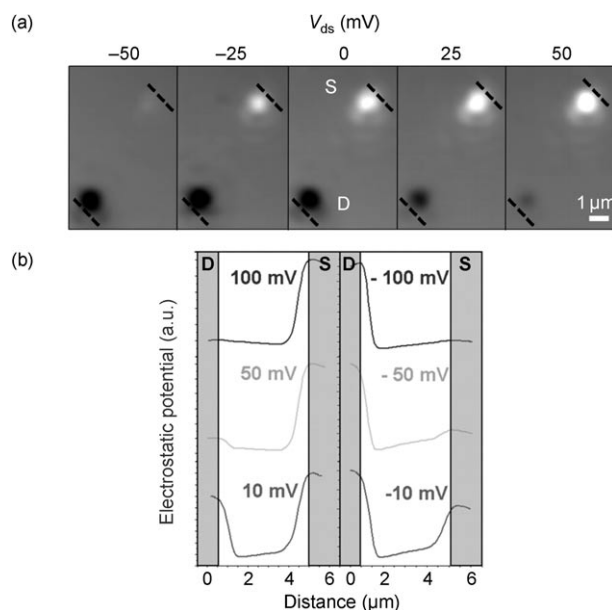

Figure 3. a) Effect of bias voltage on the photoresponse in the n-type ON state; b) CNFET electrostatic potential profiles taken along the nanotube.

CNFET band profile, we integrate the photocurrent signal along the length of the tube. This approach is justified by assuming that the photocurrent is directly proportional to the built-in electric field. In Figure 3b, the resulting qualitative electrostatic potential profiles are depicted for different bias values, with the source taken as ground and the drain being lifted (lowered) upon application of a negative (positive) potential. It follows from the line profiles that the centre of the channels remains approximately flat irrespective of the applied bias. Moreover, application of a more positive (negative) bias results in a voltage drop predominantly occurring at the source (drain). The band profile changes with increasing bias closely following the behaviour expected for the n-type unipolar operation mode of a CNFET, confirming that the charge transport through the CNT is governed by the contacts.

Finally, the effect of gate voltage on the photoresponse of biased CNFETs was investigated. To this end, a series of images similar to those in Figure 2 were recorded at an applied bias of $V_{ds} = +0.7$ V, which are collected in Figure 4a. At the starting point of $V_G = 10$ V in the n-type regime, a single lobe at the source contact is observed, in close correspondence to the situation in Figure 3a. Upon decreasing V_G, the intensity of this lobe gradually decreases and clear photocurrent signals emerge along the tube between the contacts. Around $V_G = 3.7$ V, p-type operation sets in and a single lobe emerges at the drain contact, analogous to the observation in Figure 3a. The set of SPCM images provides a complete picture of the photoconductivity in CNFETs, which is in close agreement with a previously proposed model.[17] A major conclusion is that true photoconductivity from an individual CNT is only observable in the OFF state of the device. In the ON states, the local photoresponse is similar to that obtained from a reverse-biased Schottky
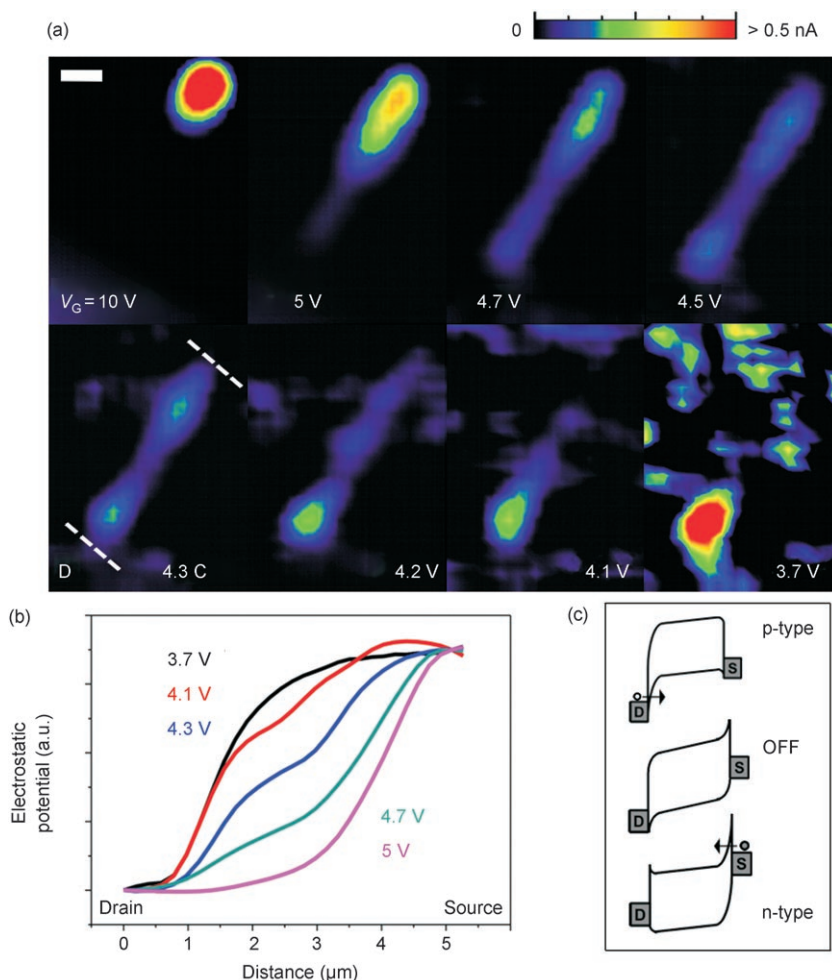
Figure 4. a) SPCM images reflecting the transition from the n- to the p-type regimes taken at $V_{ds} = 0.7$ V; b) electrostatic potential profiles obtained from the corresponding photocurrent images; c) band diagrams describing the different transport regimes of a biased CNFET.

nescence (where V_{ds} is required to be twice as high as V_G), the extracted band profiles describe the underlying scenario remarkably well.

In summary, SPCM has been demonstrated to be a highly versatile tool for CNFET characterization, which enables evaluation of the band-structure profile and the Schottky-barrier heights at the contacts in nanoscale field-effect transistors under different operating conditions. In future experiments, this technique could significantly contribute to deepen the understanding of modulations in the electronic structure of nanotube/nanowire conducting channels that arise from local defects or chemical functionalization, and thus to further enhance the performance of the corresponding devices.

Experimental Section

SWCNTs were synthesized via chemical vapour deposition (CVD), following the procedure reported by Choi et al.[19] AuPd electrical contacts (15-nm thickness) were defined on top

diode. It can be recognized from the corresponding electrostatic potential profiles in Figure 4b that in the p- (n-) type regime, the voltage drops are concentrated at the drain (source) contact, as opposed to the OFF state, in which the potential drop is distributed along the entire channel. Closer inspection of the profile at $V_G = 4.3$ V suggests that the voltage drop occurring in the vicinity of the contacts is symmetric and stronger than in the middle of the CNT. In total, the band profiles agree very well with the widely accepted model for the operating mechanism of CNFETs, wherein the band structure at the contacts is modulated by the fields induced by gate and drain-source voltages.[14] The band profiles are also consistent with the current model used to interpret electroluminescence experiments.[18] Specifically, in the OFF state, the voltage drops at the contacts are symmetric, thus leading to balanced injection of electrons and holes, followed by light emission from the centre of the devices. Upon moving away from the OFF state to the p- (n-) type regime, the voltage is found to drop mostly at the drain (source) contact, whereby hole (electron) injection is favoured. Although the drain bias used in the present experiment is not ideally suited for observing electrolumi-

the tubes using standard electron-beam lithography. Photoillumination was carried out by a HeNe laser ($E = 1.96$ eV, 0.5-μm spot size) with a focused beam intensity of ≈ 100 kW cm^{-2}. The photocurrent measurements were performed under ambient conditions on a total of 11 different devices which displayed the same principal behaviour. The figures present data gained from two specific devices, with Figures 1, 3, and 4 corresponding to sample 1, while Figure 2 belongs to sample 2.

[1] P. Avouris, *MRS Bull.* **2004**, *29*, 403.
[2] M. Freitag, Y. Martin, J. A. Misewich, R. Martel, P. Avouris, *Nano Lett.* **2003**, *3*, 1067.
[3] Z. H. Chen, J. Appenzeller, J. Knoch, YM Lin, P. Avouris, *Nano Lett.* **2005**, *5*, 1497.
[4] M. Freitag, M. Radosavljevic, Y. X. Zhou, A. T. Johnson, W. F. Smith, *Appl. Phys. Lett.* **2001**, *79*, 3326.

[5] M. Bockrath, W. Liang, D. Bozovic, J. H. Hafner, C. M. Lieber, M. Tinkham, H. Park, *Science* **2001**, *291*, 283.

[6] K. Balasubramanian, Y. Fan, M. Burghard, K. Kern, M. Friedrich, U. Wannek, A. Mews, *Appl. Phys. Lett.* **2004**, *84*, 2400.

[7] K. Balasubramanian, M. Burghard, K. Kern, M. Scolari, A. Mews, *Nano Lett.* **2005**, *5*, 507.

[8] M. Freitag, J. C. Tsang, A. Bol, D. N. Yuan, J. Liu, P. Avouris, *Nano Lett.* **2007**, *7*, 2037.

[9] S. Heinze, J. Tersoff, R. Martel, V. Derycke, J. Appenzeller, P. Avouris, *Phys. Rev. Lett.* **2002**, *89*, 106801.

[10] Y. F. Chen, M. S. Fuhrer, *Nano Lett.* **2006**, *6*, 2158.

[11] F. Leonard, J. Tersoff, *Phys. Rev. Lett.* **2002**, *89*, 179902.

[12] M. S. Marcus, J. M. Simmons, O. M. Castellini, R. J. Hamers, M. A. Eriksson, *J. Appl. Phys.* **2006**, *100*, 084306.

[13] Y. Ahn, J. Dunning, J. Park, *Nano Lett.* **2005**, *5*, 1367.

[14] J. Appenzeller, J. Knoch, V. Derycke, R. Martel, S. Wind, P. Avouris, *Phys. Rev. Lett.* **2002**, *89*, 126801.

[15] S. Rosenblatt, Y. Yaish, J. Park, J. Gore, V. Sazanova, P. L. McEuen, *Nano Lett.* **2002**, *2*, 89.

[16] R. Martel, V. Derycke, C. Lavoie, J. Appenzeller, K. K. Chan, J. Tersoff, P. Avouris, *Phys. Rev. Lett.* **2001**, *87*, 256805.

[17] K. Balasubramanian, M. Burghard, *Semicond. Sci. Technol.* **2006**, *21*, S22.

[18] M. Freitag, J. Chen, J. Tersoff, J. C. Tsang, Q. Fu, J. Liu, P. Avouris, *Phys. Rev. Lett.* **2004**, *93*, 076803.

[19] H. C. Choi, W. Kim, D. Wang, H. J. Dai, *J. Phys. Chem. B* **2002**, *106*, 12361.